Nonfrequency-Shifted Phase Conjugation by Brillouin-Enhanced Four-Wave Mixing

PAUL NARUM AND ROBERT W. BOYD

Abstract—**We present a theoretical treatment of four-wave mixing (FWM) in a Brillouin-active medium for the case in which the pump waves differ in frequency by approximately twice the Brillouin frequency shift of the medium and in which the probe-wave frequency is approximately the arithmetic mean of the frequencies of the two pump waves. Under these conditions, the conjugate wave produced by the FWM process has the desirable property of being at the same frequency as the probe. We derive the coupled amplitude equations describing this interaction. We solve these equations analytically in the limit of negligible pump depletion and find that large phase conjugate reflectivities are readily achievable. The coupled amplitude equations are solved numerically for the general case, and it is found that large power transfer from the pumps to the output wave is possible. The output wave is shown to be a nearly perfect phase conjugate of the probe wave, even far into the regime where pump depletion effects are important. Our formalism predicts the existence of a parametric instability in the propagation of the pump waves, but good performance is predicted before the onset of this instability.**

THE two principal methods for producing the phase conjugate of an optical wave are degenerate FWM [1] and stimulated Brillouin scattering (SBS) [2]. Although each of these processes is known to produce high-quality phase conjugation under certain conditions, each has certain drawbacks that limit its usefulness. Degenerate FWM leads to high-quality phase conjugation only if the two pump waves are accurately aligned to be counterpropagating and to have wavefronts that are phase conjugates of each other. Furthermore, the efficiency of the phase conjugation process is typically rather low unless the frequency of the waves is chosen so that they can resonantly excite the nonlinear medium. On the other hand, stimulated Brillouin scattering is easy to implement and has high efficiency, but leads to phase conjugation that is imperfect both in that the output is shifted in frequency with respect to the input and in that the output wavefront is only approximately the conjugate of that of the input [3]. Furthermore, since the SBS process is pumped by the signal wave, this process can never lead to reflectivities greater than 100 percent.

In this paper, we describe theoretically a new method for producing a phase conjugate wave. This method combines the desirable features of phase conjugation by degenerate FWM with the desirable features of phase conjugation by SBS, yet has none of the disadvantages mentioned above of either. The geometry for this interaction is shown in Fig. 1. The two pump waves of amplitudes E_1 and E_2 are counterpropagating and differ in frequency by 2Ω where Ω is the Brillouin frequency of the FWM medium. The probe wave of amplitude E_3 is at a frequency midway between those of the two pump waves. In Fig. 1(a) the probe wave enters the medium from the same side as the high-frequency pump wave; in Fig. 1(b) the probe enters from the same side as the low-frequency pump wave. In either case, the interaction of these three waves leads to the generation of the phase conjugate output wave E_4, whose frequency is equal to that of the probe. These four interacting waves are very strongly coupled because the nonlinear interaction is mediated by an intense acoustic wave of frequency Ω that is resonantly excited by the beating between the probe wave and the pump wave that propagates nearly antiparallel to it and by the beating between the conjugate wave and the other pump wave. We show below that this interaction can lead to the generation of the output wave with reflectivities in excess of 100 percent. Brillouin-enhanced FWM using equal-frequency pump waves has been observed by Andreev *et al.* [4] and has been discussed theoretically by Scott [5]; however, their geometry has the undesirable property that the conjugate wave is produced at a frequency other than that of the probe wave.

An important feature of the geometry considered here is that it is possible to create the low-frequency pump wave by focusing the transmitted high-frequency pump wave into a cell in which the normal SBS process occurs, as illustrated in Fig. 2. The Brillouin-active material used in the SBS generator is selected so that its Brillouin frequency is twice that of the material used in the Brillouin-enhanced FWM region. The frequency difference between the two pump waves thus has the proper value of 2Ω. Furthermore, since the backward-going pump wave is created by the SBS process, it is to good approximation a phase conjugate of the forward-going pump wave, and

Manuscript received September 23, 1986; revised January 29, 1987. This work was supported in part by the New York State Center for Advanced Optical Technology and in part by NATO under Science Fellowship 2822.

P. Narum was with the Institute of Optics, University of Rochester, Rochester, NY 14627. He is now with the Norwegian Defence Research Establishment, N-2007 Kjeller, Norway.

R. W. Boyd is with the Institute of Optics, University of Rochester, Rochester, NY 14627.

IEEE Log Number 8714410.

0018-9197/87/0700-1211$01.00 © 1987 IEEE

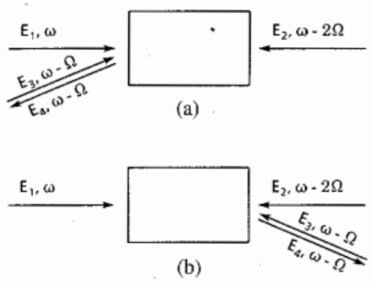

Fig. 1. The four-wave mixing (FWM) geometries considered here. The two counterpropagating pump waves E_1 and E_2 differ in frequency by twice the Brillouin frequency shift Ω of the medium. The frequencies of the probe wave E_3 and the signal wave E_4 are halfway between those of the pump waves. Both geometries lead to large reflectivities for weak probe waves, but the geometry of (a) leads to higher energy transfer when the probe is not weak.

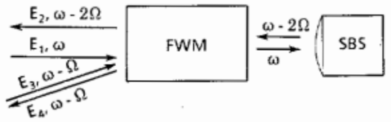

Fig. 2. Experimental setup to generate the low-frequency pump wave from the transmitted pump wave using stimulated Brillouin scattering. The SBS medium has a Brillouin frequency twice that of the FWM medium. Note that the two pump waves are automatically phase conjugates of one another.

hence the requirement that the two pump waves be phase conjugates of one another is automatically satisfied.

We describe Brillouin-enhanced FWM by generalizing the formalism used to describe the SBS process [6], [7] to the FWM geometry [5]. We assume for definiteness the geometry of Fig. 1(a), although as shown below our results can readily be modified to pertain to the geometry of Fig. 1(b). We assume that the various optical fields are linearly polarized in the same direction and can be represented within the nonlinear medium as

$$F_i(\vec{r}, t) = \tfrac{1}{2}E_i(\vec{r})\, e^{i(\vec{k}_i \cdot \vec{r} - \omega_i t)} + \text{c.c.} \qquad (i = 1, 2, 3, 4) \tag{1}$$

where $\vec{k}$ is the wave vector of wave i in the medium and ω_i is its frequency. The interference between each pair of waves leads to a density variation within the Brillouin-active medium through the process of electrostriction. We next make the usual assumptions that are used to describe the SBS process, namely, that the hydrodynamic equations may be used in their linearized form, that the phonons are strongly damped, and that the slowly varying amplitude approximation is valid. We then find that the deviation of the material density from its equilibrium value ρ_0 due to the interference between wave i and wave j is given by

$$\rho_{ij}(\vec{r}, t) = \frac{1}{16\pi} E_i(\vec{r})\, E_j^*(\vec{r}) \frac{\gamma^e |\vec{q}_{ij}|^2}{(|\vec{q}_{ij}| v)^2 - \Omega_{ij}^2 + 2i\Gamma_{ij}\Omega_j} \cdot e^{i(\vec{q}_{ij} \cdot \vec{r} - \Omega_{ij} t)} + \text{c.c.} \tag{2}$$

where $\gamma^e = \rho(\partial\epsilon/\partial\rho)_T$ is the electrostrictive constant, v is the speed of sound in the medium, Γ_{ij} is the Brillouin linewidth, $\Omega_{ij} = \omega_i - \omega_j$, and $\vec{q}_{ij} = \vec{k}_i - \vec{k}_j$. Equation (2) predicts that the amplitude of the density wave will be particularly large when the condition

$$(|\vec{q}_{ij}| v)^2 = \Omega_{ij}^2 \tag{3}$$

is satisfied. This condition holds when the interference pattern between waves i and j moves at the speed of sound in the medium. The density wave is resonantly enhanced under this condition because the electrostrictive driving term can couple effectively to a freely propagating acoustic wave. The frequency of this acoustic wave is $|\vec{q}_{ij}| v$, which is the Brillouin frequency for the interaction of waves i and j. For the geometry of Fig. 1(a), only the interference of waves 1 and 4 and of waves 2 and 3 satisfies the Brillouin resonance condition (3). We therefore will not consider the acoustic disturbance resulting from the interaction of any other pairs of waves. Since the acoustic wave vectors satisfy the condition $\vec{q}_{14} = \vec{q}_{23}$, the Brillouin frequency $\Omega = |\vec{q}_{14}| v = |\vec{q}_{23}| v$ is the same for both resonant contributions to the density grating. For generality, we allow the possibility that the incident waves do not exactly meet the Brillouin resonance condition, and hence that the frequencies of the incident waves are related by

$$\omega_2 = \omega_1 - 2\Omega + \Delta_2 \tag{4}$$

$$\omega_3 = \omega_1 - \Omega + \Delta_3 \tag{5}$$

where the detunings Δ_2 and Δ_3 are assumed to be small compared to Ω. The frequency $\omega_4 = \omega_1 + \omega_2 - \omega_3$ of the output wave is hence given by

$$\omega_4 = \omega_1 - \Omega + \Delta_2 - \Delta_3. \tag{6}$$

The density variation given by (2) leads to a variation in the dielectric constant of the medium. The scattering of the incident field from this inhomogeneity can be described in terms of a nonlinear contribution to the polarization of the medium that is given by

$$P^{\text{NL}}(\vec{r}, t) = \frac{\gamma^e}{4\pi\rho_0}[\rho_{14}(\vec{r}, t) + \rho_{23}(\vec{r}, t)]F(\vec{r}, t) \tag{7}$$

where $F(\vec{r}, t) = F_1(\vec{r}, t) + F_2(\vec{r}, t) + F_3(\vec{r}, t) + F_4(\vec{r}, t)$ is the total electric field, which is required to obey the driven wave equation

$$\nabla^2 F - \frac{n^2}{c^2}\frac{\partial^2 F}{dt^2} = \frac{4\pi}{c^2}\frac{\partial^2 P^{\text{NL}}}{\partial t^2} \tag{8}$$

where n is the refractive index. We next derive the coupled amplitude equations obeyed by the slowly varying field amplitudes by dropping from the right-hand side of (8) those terms that are not at least approximately phase matched. For simplicity, we also assume that the angle between the forward-going pump wave and the probe wave is small, and thereby obtain

$$\frac{\partial E_1^*}{\partial z} = -E_4^*(Q_{14} + Q_{23}\,e^{i\Delta kz}) \tag{9a}$$

$$\frac{\partial E_2^*}{\partial z} = -E_3^*(Q_{23} + Q_{14}\,e^{-i\Delta kz}) \tag{9b}$$

$$\frac{\partial E_3^*}{\partial z} = -E_2^*(Q_{23} + Q_{14}\,e^{-i\Delta kz}) \tag{9c}$$

and

$$\frac{\partial E_4^*}{\partial z} = -E_1(Q_{14} + Q_{23}\,e^{i\Delta kz}) \tag{9d}$$

where the coupling coefficients

$$Q_{14} = g\,\frac{nc}{8\pi}\,E_1^* E_4 \tag{10a}$$

and

$$Q_{23} = g\,\frac{nc}{8\pi}\,E_2 E_3^* \tag{10b}$$

are proportional to the amplitudes of the density waves driven by the beating of waves 1 and 4 and of waves 2 and 3, respectively. The coefficient

$$g = \frac{(\gamma^e\omega)^2}{4\Gamma nvc^3\rho_0}\,\frac{1}{1 + i(\Delta_3 - \Delta_2)/\Gamma} \tag{11}$$

reduces to the line-center amplitude gain coefficient for the normal SBS process [7] for the case $\Delta_3 = \Delta_2$. The wave vector mismatch $\Delta k = 2n\Omega/c$ is the intrinsic phase mismatch of Brillouin-enhanced FWM in the geometry of Fig. 1.

In the limit in which the complex field amplitudes of the pump waves can be assumed to be constant, the coupled amplitude equations (9c) and (9d) for the probe and conjugate wave amplitudes can be solved analytically. We find that the amplitude reflectivity $r = E_4^*(0)/E_3(0)$ for the boundary condition $E_4(L) = 0$ is given by

$$r = \frac{a^+a^-}{2\sqrt{a_1a_2}}\,\frac{\exp\left[(a^+ - a^-)L/2\right] - 1}{a^- - a^+\exp\left[(a^+ - a^-)L/2\right]}\,\frac{E_1^*E_2^*}{|E_1E_2|} \tag{12a}$$

where

$$a_i = -gI_i \qquad (i = 1, 2) \tag{12b}$$

$$a^\pm = a_1 - a_2 + i\Delta k \pm \left[(a_1 - a_2 + i\Delta k)^2 + 4a_1a_2\right]^{1/2} \tag{12c}$$

and

$$I_i = \frac{nc}{8\pi}\,|E_i|^2. \tag{12d}$$

For the case in which the probe wave is nearly copropagating with the low-frequency pump wave [as in Fig. 1(b)] the appropriate boundary condition is $E_4(0) = 0$, and the reflectivity now defined as $E_4^*(L)/E_3(L)$ is still given by the set of equations (12). We shall show later that this symmetry no longer holds for the case in which pump depletion occurs. In this more general case, the geometry of Fig. 1(a) yields the higher transfer of energy from the pump waves into the output wave, and for this reason, the formulas (9)–(11) have been written to apply explicitly to the geometry shown in Fig. 1(a).

The analytic results of (12) are formally identical to those obtained by Scott [5] for his different choice of input frequencies. As in that case, our expression for the predicted reflectivity simplifies dramatically under certain limits. In the limit in which the phase mismatch can be neglected, that is, the limit $|\Delta k| \ll |a_1 - a_2|$, the amplitude reflectivity approaches the value

$$r = (I_1I_2)^{1/2}\,\frac{\exp\left[g(I_1 + I_2)L\right] - 1}{I_1 + I_2\exp\left[g(I_1 + I_2)L\right]}\,\frac{E_1^*E_2^*}{|E_1E_2|} \tag{13}$$

for either the geometry of Fig. 1(a) or of Fig. 1(b). If in addition we consider the case in which the Brillouin resonance condition $\Delta_2 = \Delta_3$ is satisfied so that the parameter g of (11) is a real positive number and in which the input intensities are sufficiently large that $g(I_1 + I_2)L \gg 1$, the amplitude reflectivity r is seen to approach the value $(I_1/I_2)^{1/2}$ [5]. Hence, for the geometry of Fig. 1(a), the reflectivity is greater than unity if the pump wave that copropagates with the probe is stronger than the other pump wave, whereas for the geometry of Fig. 1(b), the reflectivity is greater than unity if the counterpropagating pump wave is the stronger.

In Fig. 3, we display graphically the nature of the solution given by (12) for three different values of the cell length L and under the assumption that the Brillouin resonance condition $\Delta_2 = \Delta_3$ is satisfied. The power reflectivity $|r|^2$ is plotted as a function of the normalized intensity I_1L of the forward-going pump wave for several different values of the ratio $R = I_1/I_2$ of the pump intensities. For definiteness, we use those values of the material parameters that are appropriate for the case of Brillouin-enhanced FWM in carbon disulfide at a wavelength of 0.53 μm, that is, $\Delta k = 5.25$ cm^{-1} and $g = 0.075$ cm/MW. It is seen from these plots that large reflectivities are readily obtained. We note that for large intensities, the reflectivity approaches the value I_1/I_2, as expected [5]. For the shortest cell length shown, wave vector mismatch effects are unimportant and the reflectivity increases monotonically with increasing pump intensity, whereas for longer cell lengths phase mismatch effects become important and the behavior becomes more complicated.

It might be difficult experimentally to control the input frequencies well enough that the Brillouin resonance condition is exactly met. In Fig. 4 we show the dependence

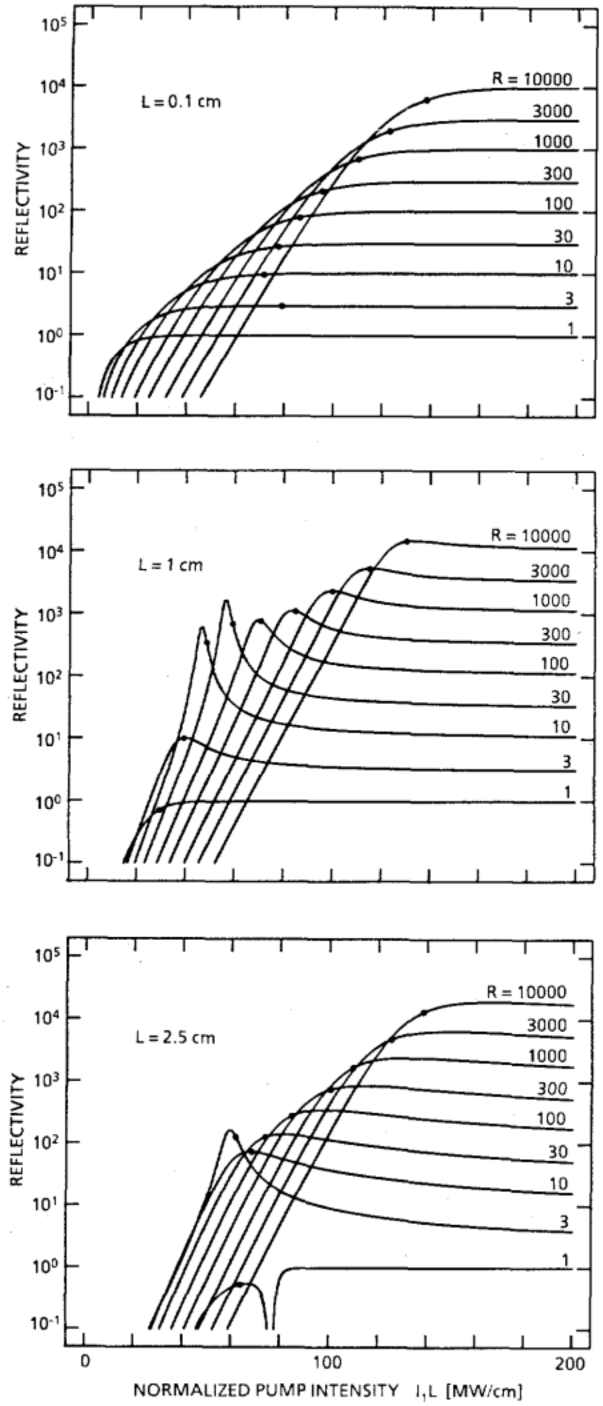

Fig. 3. Reflectivity of the Brillouin-enhanced FWM process plotted as a function of the normalized pump intensity for several different values of the cell length L and the ratio $R = I_1/I_2$ of the intensities of the two pump waves. We assume the case of exact Brillouin resonance ($\Delta_3 - \Delta_2$), and we use the values of the gain coefficient and wave vector mismatch for the case of CS_2 as the nonlinear medium and a wavelength of 0.53 μm. The small dots mark the intensity at which an instability in the propagation of the pump waves occurs.

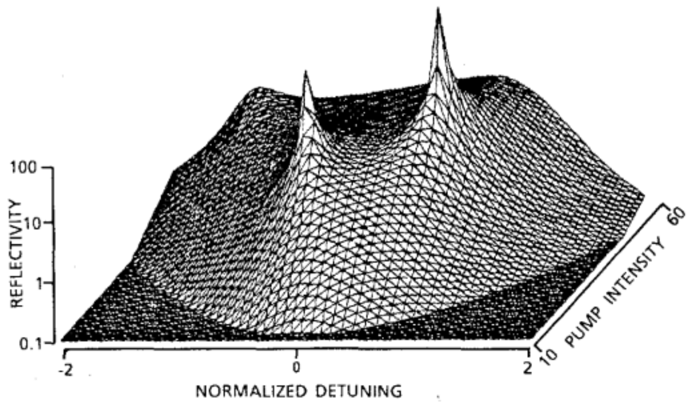

Fig. 4. Reflectivity plotted as a function of the normalized detuning $(\Delta_3 - \Delta_2)/\Gamma$ from the Brillouin resonance end of the pump intensity I_1 in megawatts per centimeter for a cell length of 2.5 cm and a pump beam intensity ratio of $R = 40$, for the case of CS_2 as the nonlinear medium and wavelength of 0.53 μm.

of the power reflectivity on the detuning $\Delta_2 - \Delta_3$ from the exact Brillouin resonance, for a cell length of 2.5 cm and a pump intensity ratio of $R = 40$. For the case of low input intensities, the tuning curve has the same shape as the Lorentzian-shape Brillouin resonance of (11). As the pump intensities are increased gradually, the tuning curve broadens and develops a secondary peak that moves initially to negative detunings and later to positive detunings. At the peaks of Fig. 4, the reflectivity formally becomes infinite. This divergence is the origin of a parametric instability in the FWM process. The maximum value of the pump intensity is limited by the onset of this instability, which occurs when the complex denominator in (12a) first becomes zero [8]. In the limit of an interaction region sufficiently short that $\Delta kL << 1$, Δk can be neglected in (12), and the instability is seen to occur for a forward pump intensity given by

$$I_1 = R\,\frac{\pi^2 + (\ln(R))^2}{Lg_0 \ln(R)(1 + R)} \tag{14}$$

and at a detuning from the Brillouin resonance of $\Delta_3 - \Delta_2 = \pm\pi\Gamma/\ln(R)$. More generally, the onset of this instability is determined numerically by finding the lowest value of the intensity I_1 for which (12) becomes infinite for some value of the detuning $\Delta_3 - \Delta_2$ from the Brillouin resonance. We allow the detuning to be arbitrary because when the reflectivity is infinite, an instability can develop even in the absence of an input field. The location of this instability is marked by a small dot on each curve shown in Fig. 3. Note that very large reflectivities can be obtained before this instability is reached. The threshold for SBS (taken as the condition that the exponential gain be equal to 30) due to the E_1 pump wave in the absence of the E_2 pump wave occurs in all cases at the value 200 MW/cm^2 of the normalized pump intensity. The threshold for instability is seen to be significantly lowered by the presence of the counterpropagating pump wave under most circumstances. Of the cases illustrated, only for $L = 0.1$ cm and $R = 1$ is the threshold raised.

Since the reflectivities in Brillouin-enhanced FWM can be very large, it is easy to operate in a regime where significant pump depletion occurs. Pump depletion effects are important both because they limit the fraction of the pump energy that can be transferred to the signal wave and because they can limit the extent to which the signal wave is the phase conjugate of the probe wave. In order to treat pump depletion effects, it is necessary to solve the entire set of coupled equations (9). Analytic solutions to the complete set of coupled equations describing FWM in photorefractive materials [9] and in Kerr media [10] have recently been presented. However, we have been unable to find an analytic solution to our set of equations because the nature of the coupling is different in our case. We have thus solved the set of equations numerically. Since the boundary conditions for two of the waves are imposed at $z = 0$, whereas the boundary conditions for the other two waves are imposed at $z = L$, the equations constitute a two-point boundary value problem. We have solved these equations using a shooting and matching method [11]. To ensure the numerical accuracy of our solution, we have verified that the relevant constants of the motion

$$C_1 = I_1 - I_4 \tag{15a}$$

and

$$C_2 = I_2 - I_3 \tag{15b}$$

given by the Manley–Rowe relations are conserved at all points within the interaction volume to better than 0.3 percent. Sets of equations describing FWM are known to lead to multivalued solutions [9], [10]. We have not studied the possibility of multivalued solutions to our set of equations. Instead, we have determined only that solution which connects adiabatically to the low-probe-intensity solution as the probe intensity is increased gradually. However, we believe that our solutions are stable because small changes in our input parameters lead to only small changes in the output. We have performed such calculations using a variety of cell lengths. We find that the best results are obtained when the input intensities are as large as possible while avoiding the threshold for instability, when the cell is sufficiently short that wave vector mismatch effects are nearly negligible, and when using the geometry of Fig. 1(a) instead of that of Fig. 1(b). The geometry of Fig. 1(a) leads to a larger energy transfer than that of Fig. 1(b) because for Fig. 1(a) the output wave experiences Brillouin gain through its interaction with the forward-going pump wave, whereas for Fig. 1(b) the output wave is attenuated by its interaction with the backward-going pump wave. Typical results are shown in Fig. 5 for a cell length of 0.1 cm and pump beam intensity ratios of 10, 30, 100, and 300. The pump intensities are chosen to be just below the onset of instability, and are given by $I_1 = 720$, 766, 860, and 967 MW · cm^{-2}, respectively. Fig. 5(a) shows the fraction of the total pump wave energy that is transferred to the signal wave plotted as a function of the probe intensity normalized in such a manner that all of the curves initially have the same slope. The curves are hence normalized in terms of the unsaturated reflectivities, which are given for the four cases by 9.56, 26.36, 78.82, and 217.4, respectively. Note that the reflectivity saturates less rapidly through the use of a lower pump intensity ratio and that more than 40 percent

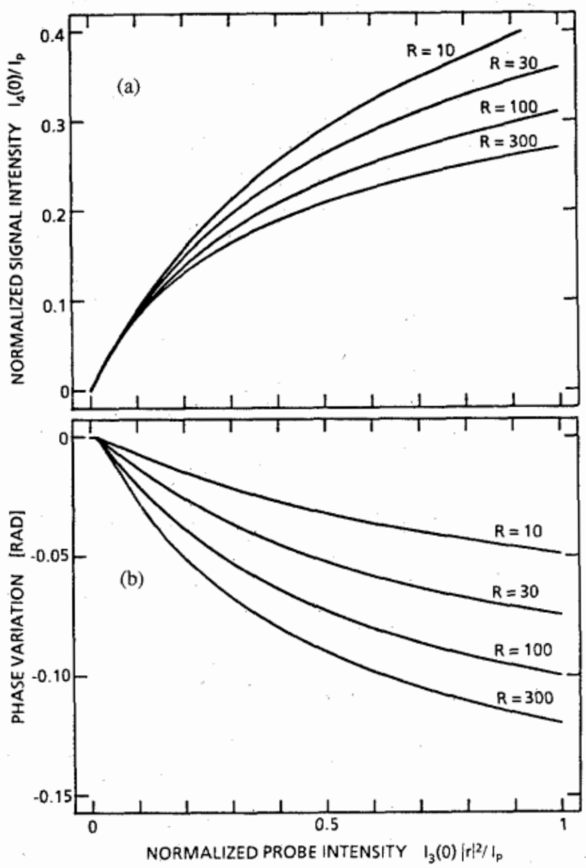

Fig. 5. (a) Energy transfer characteristics in the pump depletion regime. The fraction of the total input pump intensity I_P that is transferred to the signal wave is plotted as a function of the probe intensity, normalized in such a way that all of the curves have the same slope for low intensities. In each of the illustrated cases, the pump intensity is just below the threshold for instability. (b) Variation of the phase of the signal wave plotted as a function of the probe intensity, for the same cases as illustrated in (a).

energy transfer is possible. In order for the signal wave to be the true phase conjugate of the probe wave, it is necessary that the signal intensity depend linearly on the probe intensity and that the phase shift upon reflection not depend upon the probe intensity. We see from Fig. 5(a) that the transfer characteristics are more nearly linear for low pump intensity ratios, implying that high-quality phase conjugation consistent with high energy transfer is best achieved through the use of a low pump intensity ratio. Of course, this enhanced performance in terms of the linearity of the transfer characteristics and the energy transfer efficiency is accompanied by a decrease in the unsaturated reflectivity. Fig. 5(b) shows the variation in the phase of the signal wave as the probe intensity is increased. Note that even in the worst case shown this variation corresponds to less than 1/50 of a wave of aberration of the phase front of the signal wave, and that the performance is improved through the use of a lower pump intensity ratio.

In conclusion, we have presented a theoretical description of Brillouin-enhanced FWM in a new geometry for which the probe and signal waves have the same frequency. We find that high reflectivity, large energy transfer from the pump waves, and high-quality phase conjugation are possible, even in the pump depletion regime.

Note added in proof: We have recently completed an experimental investigation that verifies many of the predictions presented here. An account of this investigation, entitled "Non-frequency-shifted, high-fidelity phase conjugation with aberrated pump waves by Brillouin-enhanced four-wave mixing," by M. D. Skeldon, P. Narum, and R. W. Boyd, is scheduled for publication in the May 1987 issue of *Optics Letters*.

Acknowledgment

The authors gratefully acknowledge useful discussions with M. D. Skeldon.

References

[1] R. W. Hellwarth, "Generation of time-reversed wave fronts by nonlinear refraction," *J. Opt. Soc. Amer.*, vol. 67, no. 1, pp. 1-3, 1977.
[2] B. Ya. Zel'dovich, V. I. Popovichev, V. V. Ragul'skii, and F. S. Faizullov, "Connection between wave fronts of the reflected and exciting light in stimulated Mandel'stham–Brillouin scattering," *Sov. Phys. JETP Lett.*, vol. 15, pp. 109–113, 1972.
[3] N. B. Baranova, B. Ya. Zel'dovich, and V. V. Shkunov, "Wavefront reversal in stimulated light scattering in a focused spatially inhomogeneous pump beam," *Sov. J. Quantum Electron.*, vol. 8, pp. 559–566, 1980; see also, R. H. Lehmberg, "Numerical study of phase conjugation in stimulated backscatter with pump depletion," *Opt. Commun.*, vol. 43, pp. 369–374, 1982.
[4] N. F. Andreev, V. I. Bespalov, A. M. Kiselev, A. Z. Matveev, G. A. Pasmanik, and A. A. Shilov, "Wavefront inversion of weak optical signals with a large reflection coefficient," *Sov. Phys. JETP Lett.*, vol. 32, pp. 625–629, 1980.
[5] A. M. Scott, "Efficient phase conjugation by Brillouin enhanced four wave mixing," *Opt. Commun.*, vol. 45, pp. 127–132, 1983; see also, A. M. Scott and M. S. Hazell, "High-efficiency scattering in transient Brillouin-enhanced four-wave mixing," *IEEE J. Quantum Electron.*, vol. QE-22, pp. 1248–1257, 1986.
[6] W. Kaiser and M. Maier, "Stimulated Rayleigh, Brillouin, and Raman spectroscopy," in *Laser Handbook, Vol. 2*, F. T. Arrechi and E. O. Shulz-Dubois, Eds. Amsterdam, The Netherlands: North-Holland, 1972, ch. E2, pp. 1078–1150.
[7] P. Narum, M. D. Skeldon, and R. W. Boyd, "Effect of laser mode structure on stimulated Brillouin scattering," *IEEE J. Quantum Electron.*, vol. QE-22, pp. 2161–2167, 1986.
[8] B. Ya. Zel'dovich and V. V. Shkunov, "Characteristics of stimulated scattering in opposite pump beams," *Sov. J. Quantum Electron.*, vol. 12, pp. 223–225, 1982.
[9] M. Cronin-Golomb, J. O. White, B. Fischer, and A. Yariv, "Exact solution of a nonlinear model of four-wave mixing and phase conjugation," *Opt. Lett.*, vol. 5, pp. 313–315, 1982.
[10] R. Lytel, "Pump depletion effects in nonlinear degenerate four-wave mixing in Kerr media," *J. Opt. Soc. Amer. B*, to be published.
[11] W. H. Press, B. P. Flannery, S. A. Teukolsky, and W. T. Vetterling, *Numerical Recipes: The Art of Scientific Computing.* Cambridge, England: Cambridge Univ. Press, 1986.

Paul Narum was born in Toten, Norway, on March 9, 1951. He received the Sivilingnioer degree in electrical engineering from the Norwegian Institute of Technology in 1976.

From 1976 to 1979 and from 1981 to 1985 he was at the Norwegian Defence Research Establishment developing military E-O systems. In 1980 he was a Visiting Research Associate at the Institute of Optics, University of Rochester, Rochester, NY, and since 1985 he has been a Research Associate at the Institute of Optics. His present research interests include phase conjugation by stimulated scattering and four-wave mixing, quantum optics, and new materials for nonlinear optics.

Robert W. Boyd received the B.S. degree in physics in 1969 from the Massachusetts Institute of Technology, Cambridge, and the Ph.D. degree in physics in 1977 from the University of California at Berkeley.

He was appointed Assistant Professor in 1977 and Associate Professor in 1982 at the Institute of Optics of the University of Rochester, Rochester, NY. His research interests include the study of nonlinear optical interactions and the use of phase conjugation techniques in the development of laser systems.

Dr. Boyd is the author of *Radiometry and the Detection of Optical Radiation* (New York: Wiley, 1983), is a Coeditor of *Optical Instabilities* (Cambridge, England: Cambridge Univ. Press, 1986), and has published approximately 60 research papers.